620 *Bull. Korean Chem. Soc., Vol. 13, No. 6, 1992*

Jin Chun Woo et al.

21. J. Herbich, Z. R. Grabowski, H. Wojtowicz, and K. Golankiewicz, *J. Phys. Chem.*, **93**, 3439 (1989).
22. W. Rettig and G. Wermuth, *J. Photochem.*, **28**, 351 (1985).
23. Z. R. Grabowski, K. Rotkiewicz, A. Siemiaczuk, D. J. Cowley, and W. Bauman, *Nouv. J. Chim.*, **3**, 443 (1979).
24. W. Rettig and W. Zander, *Ber. Bunsen-Ges. Phys. Chem.*,

87, 1143 (1983).
25. D. W. Anthon and J. H. Clark, *J. Phys. Chem.*, **91**, 3530 (1987).
26. Y. Wang and K. B. Eisenthal, *J. Chem. Phys.*, **77**, 6076 (1982).

Study of the Optimization and the Depth Profile Using a Flat Type Ion Source in Glow Discharge Mass Spectrometry

Jin Chun Woo*, Hyo Jin Kim[†], Heoung Bin Lim, Dae Won Moon, and Kwang Woo Lee

Inorganic Analytical Chemistry Lab., Korea Research Institute of Standards and Science, Taejon 305-606
[†]Department of Pharmacy, Dong Duck Women's University, Seoul 136-714
Received May 12, 1992

The analytical performance of glow discharge mass spectrometer (GD-MS), using a flat type ion source is discussed. The efficiency of ion extraction was maximized at the distance between anode and cathode of 6 mm. At the operation condition of 4 mA, −1000 volt, and 1 mbar for the source, the optimum voltages for sampler and skimmer were 40 volt and −280 volt, respectively. The intensities of Cu, Zn, and Mn were increased as a function of square root of current approximately. Korea standard reference materials (KSRM) were tested for an application study. The detection limits of most elements were obtained in the range of several ppm at the optimized operating condition. The peaks of aluminum and chromium were interfered by those of residual gases. The depth profile of nickel coated copper specimens (3, 5, 10 μm thickness) were obtained by plotting time versus intensities of Ni and Cr after checking the thickness of nickel coated using a scanning electron microscope (SEM). At this moment, the sputtering rate of 0.2 μm/min at the optimum operating condition was determined from the slope of the plot of time to the coating thickness. The roughness spectra of specimen's crater after 16 min, discharge were obtained using a Talysuf5m-120 roughness tester as well.

Introduction

As one of the inorganic analytical techniques, the glow discharge mass spectrometry (GD-MS) has been studied for a long time. The glow discharge technique is simple because a bulky solid sample can be directly analyzed without any sample preparation and free from the concommitant interference due to its unique plasma generation mechanism, i.e., sputtering, not thermal process. Even though, the glow discharge technique has the recognition as a relatively very old, compared with other plasma sources, it has many attentions from analytical scientists for an ultimate atomic spectrometer. Its application field is expanding quickly owing to the developmemt of Radio Frequency Glow Discharge Source Mass Spectrometry (RF-GDMS) which makes it possible to analyze the nonconducting samples. Marcus et al.[12] use the 13.56 MHz RF generator to supply the discharge operating potential and the electrically insulating material such as glasses and ceramics were analyzed. The operating pressure of RF-GD is 100-500 mTorr which is relatively lower than that of conventional DC-GD of 1-10 Torr.

Also, Glow Discharge Source has been increasingly applied for studying the chemical composition of solid surfaces and thin film systems. This is due to the minimal sample preparation requirements, good depth resolution, and wide dynamic range. However, most of researches for the in-depth analysis

with the glow discharge have been studied by the optical method. Belle et al.[3] analysed the metal alloys in depths of 0.1 to 40 μm with a glow discharge source for optical emission spectrography. Greene et al.[4-7] determined boron impurity profiles in silicon, measuring the concentration and distribution of constituents in semiconductor films, and the depth information in solid samples. Waitlevertch et al.[8] operated a glow discharge with a constant dc mode or a square wave dc mode, but better repriducibility and accuracy have been achived with the square-wave dc mode. Pons-Corbeau et al.[9,10] studied the quantitative determination of variations of composition in galvanized coatings and for an estimation of the enrichments on the surface of annealed extra mild steel sheets with GD-OES. They also show that the emission yield of an element is independent of the matrix although particular phenomena can affect the apparent experimental values. Bengton[11] investigated the variation in intensity of Ar I lines in order to exclude the influence of the sample sputtering rate, and compared with the sample sputtering rate. He concluded that the number density of the sample atom in the plasma saturates with increasing voltage. Nickel et al.[12] applied the various glow discharge mode to find optimum conditions for the transformation of intensity-time profiles into concentration-depth dependencies using the alloy matrix as a reference. Element concentrations were calcul-
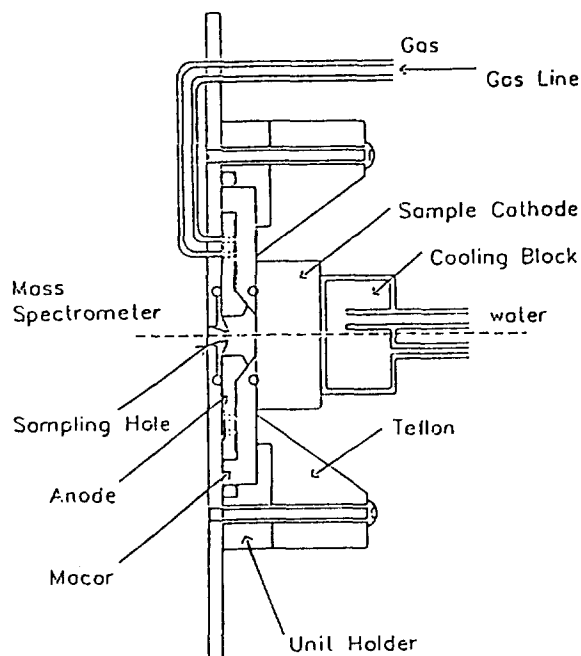
Study the Depth Profile by GD Mass

Bull. Korean Chem. Soc., Vol. 13, No. 6, 1992 621

Figure 1. Schematic diagram of the modified flat type ion source.

Figure 2. Schematic diagram of Grim (a) and flat (b) type ion source.

ated from intensity ratios, corrected with respect to sputtering rates and discharge current ratios.

Hecq *et al.*[13] analysed copper targets covered by a sequence of thin metallic films by glow discharge mass spectrometry, and showed that the sensitivity is inversely proportional to the ion mass. Straaten *et al.*[14] measured the etching rate of Mo samples in a plannar GD as a function of applied power density (0-10 W/cm^2) and pressure of 365-750 mTorr, and compared with calculated values obtained by modeling of a one dimentional planar glow discharge. They showed that satisfactory correlation between the measured and calculated etching rates predicted the diffusion profiles of sputtered neutrals. In this study, the distance between the anode and the cathode, sampler voltage, skimmer voltage, discharge current have been optimized to study the in-depth analysis with the modified flat type ion source.

Experimental

Apparatus. A diagram of glow discharge mass spectrometer system used in this experiment was described in the previous paper[15,16]. The whole apparatus is based on the differential pumping system for the dual stage, the first stage of the interface between the ion source and mass analyzer, and the second stage of the ion optics, electrostatic energy analyzer (cyclindrical mirror analyzer), quadrupole mass filter and channel electron multiplier. The differential pumping system was made up by two diffusion pumps (Veeco Model VR-300, pumping speed of 600 L/sec and 170 L/sec) with forepumps. The typical operating pressures of the first stage and the second stage (mass analyser chamber) were maintained at 1×10^{-4} mbar and 1×10^{-6} mbar, respectively.

The ions produced in the ion source were extracted into the first stage through the sampler with the aperature of 0.4 mm, and entered the mass analyzer through a skimer
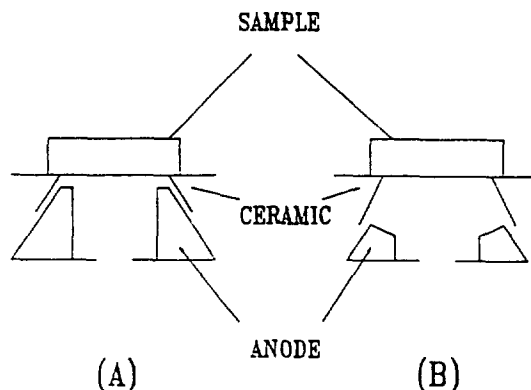
cone of 0.7 mm diameter. The potentials of sampler and skimmer were adjustable to optimize the extraction efficiency of ions from the source. The energy analyzer, the quadrupole mass filter were controlled by Spectralab SXP 300, VG instruments.

Ion Source. A flat type ion source was modified to have the 3.0 mm distance between the anode and the surface of sample to improve the long term discharge stability as shown in Figure 1. The glow discharge cell made of stainless stell and macor, was electrically isolated from the ground. The discharge voltage could be varied between 400 and 1500 volt using a regulated DC power supply (Imace Engineering Co., Korea). By the adjustment of gas pressure, the discharge current could be varied from 1 to 50 mA because the choice of flow rate defined the current for a given voltage. The feeding rate of argon as working gas could be controlled by a valve control unit (Model RVG040, Balzers). The discharge power supply was floated to the ion accelerating voltage of 0-50 VDC and 200 mA DC power supply (HP 6218B) as described previously.

The sampler as an anode was a cone shape with a 0.4 mm hole in diameter, and the height of sampling cone defined the distance between the cathode and extraction hole. The skimmer with the 0.7 mm diameter hole was positioned at the distance of 5 mm behind the ion exit orifice. The distances between the surface of sample and the anode are 0.2 mm in Figure 2(a) (Grimm type) and 3 mm in Figure 2(b) (Flat type).

Results and Discussion

Effect of the Distance of Sampling Hole. The effect of the distance between sample (cathode) and extraction hole was studied for two types of ion source in Figure 3. It is important to note that the position of sampling cone determined the chemical environments of ions to be extracted. It indicates that the choice of sampling position directly affects the extraction efficiency and the signal to background ratio. In this experiment, Cu and Ar ion signals are maximized at 6 mm distance in flat type ion source, as shown in Figure 3, whereas the optimum distance in Grimm type ion source is less than that of flat type. The shortening of negative glow region in the Grimm type is believed to the space restriction of discharge. The following studies are performed
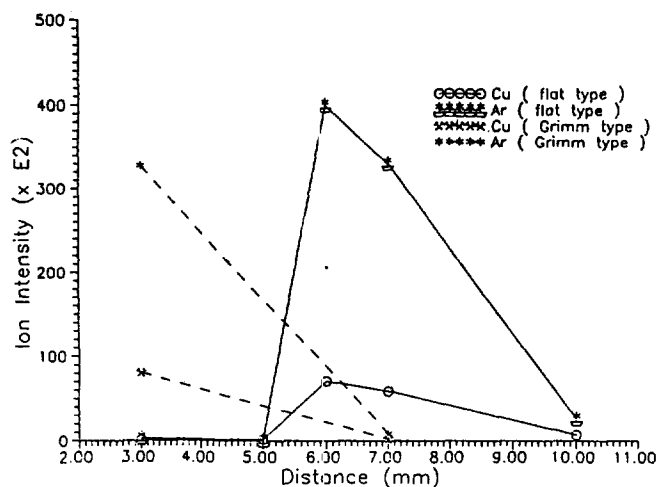
Figure 3. Effect of distance between sample and extraction hole on the ion intensities for the Grim and the flat type ion source.
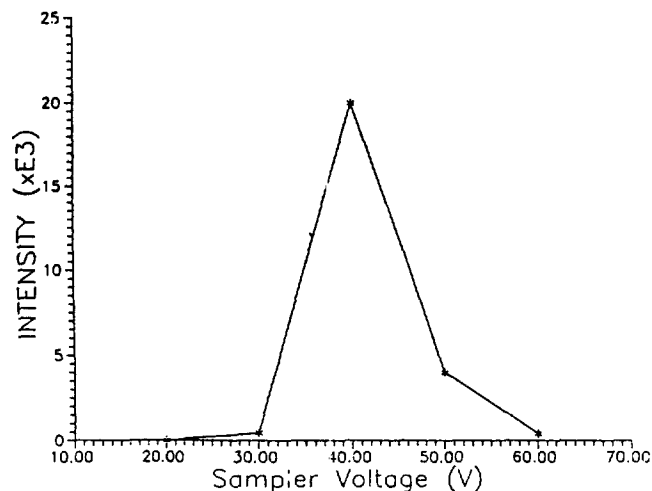

Figure 4. Effect of sampler voltates on ^{55}Mn ion intensity (-1000 V discharge voltage, 4 mA discharge current, -280 V skimmer voltage).

Figure 5. Effect of skimmer voltage on ion intensities of three elements with copper alloy sample (-1000 V discharge voltage, 4 mA discharge current, 40 V sampler voltage).

Figure 6. Characteristic curves of the voltage-current at various pressure.

using flat type ion source.

Optimization Study for Flat Ion Source. In order to optimize the operation condtions for ion extraction process, the voltages of sampler and skimmer and adjusted while the analyte signals are monitored at 4 mA and -1000 volt. The argon ion signal was maximized at sampler voltage of 40 volt. As shown in Figure 4, Ar ion signal is very sensitive to the sampler voltage. To obtain the optimum skimmer voltage, the KSRM 1126 containing Cu (62.6%), Zn (29.9%), and Mn (2.9%) is analysed at the discharge current of 4 mA, the discharge voltage -1000 volt, and the sampler voltage of 40 volt. Optimum ion signals of Cu, Zn and Mn were obtained at the skimmer voltage of -280 volt, as shown in Figure 5.

Characteristic curves of voltage-current at various pressures are shown in Figure 6. It is certain that in the current increased with the discharge voltage applied, and the increament of current is sharper at the higher pressure, rather than lower pressure, as expected. While the discharge current was increased, the signals of Cu, Zn, and Mn were
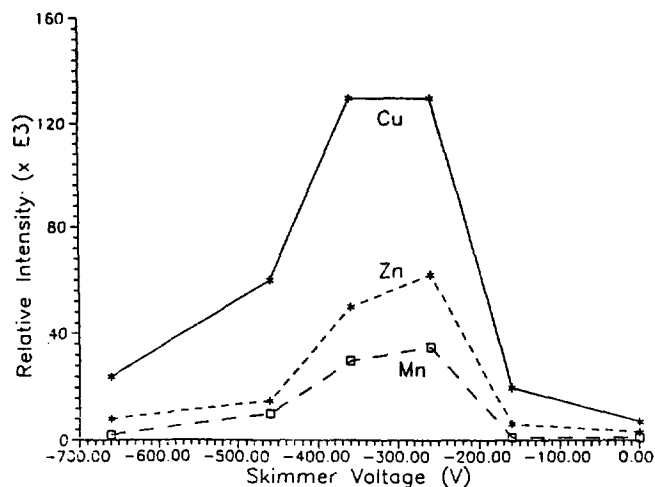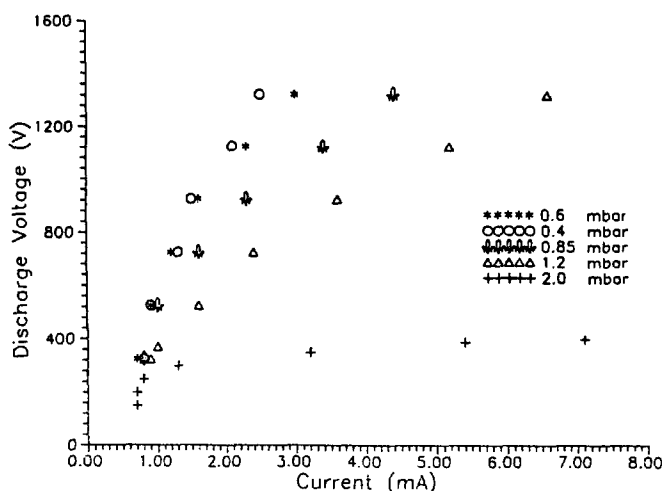
increased as well (Figure 7). The ion signals of analytes are sharply increased from the beginning, but the slopes of the increament were reduced after 4 mA. In addition, it was found that the higher current caused severe contaminations of the cell due to the deposition of the sputtered particles.

As a result, the optimized operating conditions in this experiments are 40 volt for sampler voltage, -280 volt for skimmer voltage, and 4 mA for the discharge current. It is general to say that the overall trend in the flat type ion source is similar to the pin type ion source which was discussed in the previous paper[16]. Additionally, the better stability was observed in the flat type ion source, compared to the Grimm type.

Mass Spectrum and Calibration. Mass spectrum for the copper alloy, KSRM 1126 in the mass range of 1 to 100 amu was obtained as shown in Figure 8, in order to figure out the possibility of quantitative analysis of conducting samples using this system. Strong ion signals of ^{40}Ar, ArH, Ar^{2+} and Ar$_2{}^+$ are shown from the figure. The peaks of major elements in the sample, Cu of 62.6% and Zn of 29.9%, and

Study the Depth Profile by GD Mass

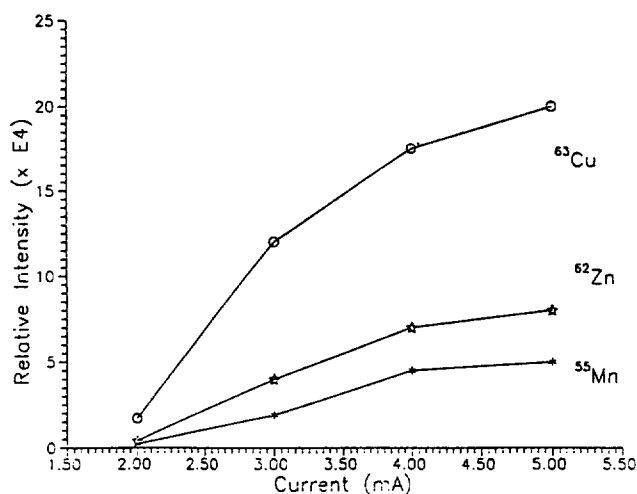*Bull. Korean Chem. Soc., Vol. 13, No. 6, 1992* 623

Figure 7. Effect of discharge current on ion intensity of three elements with copper alloy sample.
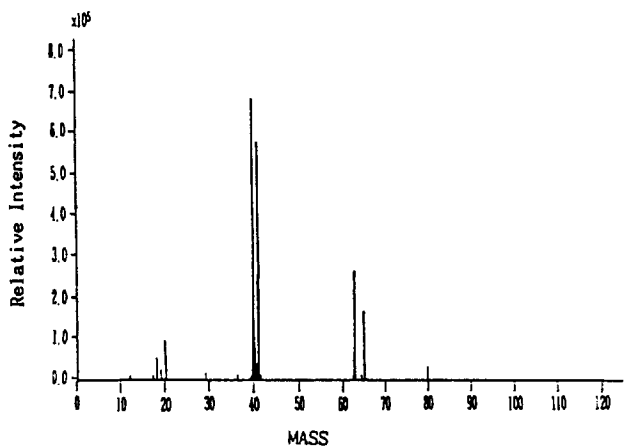

Figure 8. GD/MS spectrum of pure copper base material (4 mA discharge current, −1000 V discharge voltage).
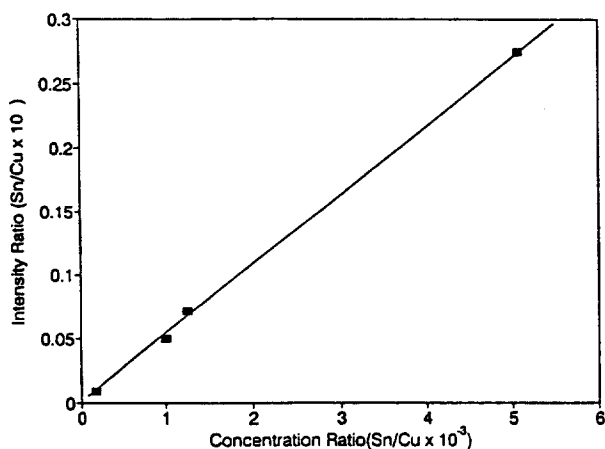

Figure 9. Calibration curve for Tin.

their isotopes are shown in the figure as well. The peaks of other elements in the KSRM 1126, Al (3.01%), Fe (0.037 %), Sn (0.011%), Ni (0.317%), Mn (2.84%), Cr (0.090%), and Si (1.23%) are observed in the spectrum. For the quantitative analysis, the calibration curves are obtained for Fe, Ni, Sn,
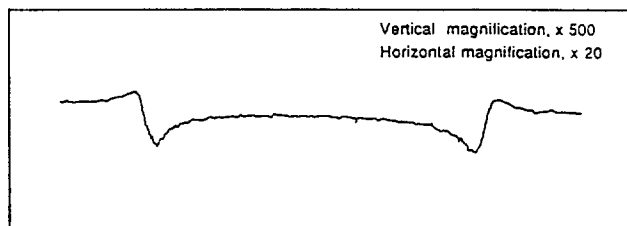

Figure 10. Roughness of specimen's crater after 16 min discharge (by Talysurf5m-120 riughness tester).
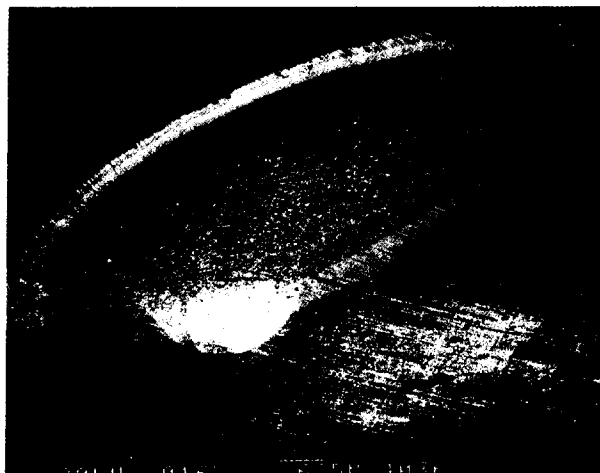

Figure 11. SEM image for copper sample after 4 hour sputtering (4 mA discharge current, −1000 V discharge voltage).

Mn, Al, and Cr using KSRM 1121, 1122, 1123, 1124, 1125 and 1126. The calibration curve for Sn, for an example, is plotted as shown in Figure 9. From the figure, the concentration ratio means the ratio of the concentration of Sn to that of Cu, and the intensity ratio represents the ratio of the intensity of Sn to that of Cu in mass spectra. The calculated limit of detection are 2 ppm for Fe, Ni, Mn and Al, 0.9 ppm for Zn, 1 ppm for Cr, and 15 ppm for Sn. It should be noted that the limits of detection calculated are not obtained from integrated signal intensity but single scan. Molecular interference were also observed due to the presence of impurities in the Ar gas.

Study of Depth Profile. One of the main advantages of GD-MS over ICP-MS is the ability of depth profiling for the bulky solid sample. The profile of the prepared samples, *i.e.*, nickel coated copper, after the sputtering for 16 min using a Talysuf5m-120 roughness tester, is shown in Figure 10. From the figure, the uneveness of sputterred spot indicate that it suffers from a serious problem of erratic ion production in the sample. This kind of inhomogeneous sampling could seriously deteriorate the resolution in the depth profiling study. It is reported that the electric filed due to the voltage applied to the cathode and anode affects the shape of the crater. According to the study of Bengtson[11], the longer distance between cathode and anode and the lower pressure in the cell could improve the crater shape. Even though the effects of the voltage and the distance on the shape of crater were not performed, the phenomena of the formation of erratic crater could be more complicated than the understood, because the operating conditions including
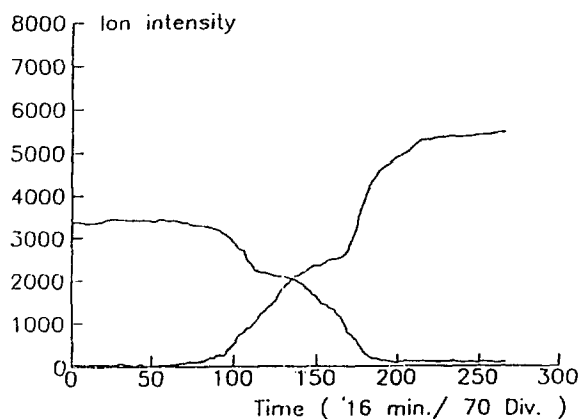
Figure 12. Analysis of nickel coated copper sample (4 mA discharge current, −1000 V discharge voltage).
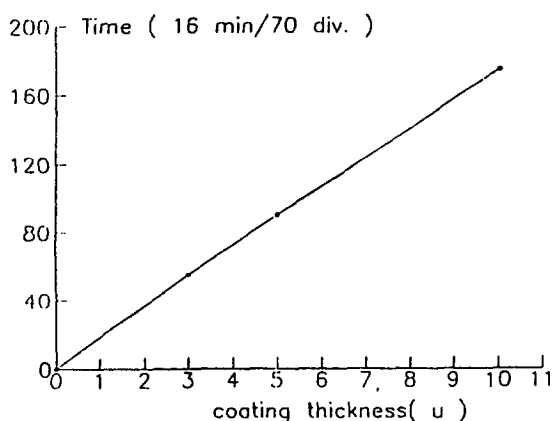

Figure 13. Coating thickness *vs.* sputtering time curve (3, 5, 10 μm nickel coated copper).

pressure and voltage meets the optimum condition suggested. The picture taken by a SEM proves the existance of the erratic shape of crater clearly, as shown in Figure 11. From the picture, the shapes of concave and convex in the levels of the flat surface and sputtered spot at the rim of the crater are seen.

Figure 12 is showing the intensity changes of nickel and copper for the time duration of an hour. First, the only nickel signal appeared without copper, then the mixed stage for nickel and copper, and finally the only copper signal was observed. One of the reasons for the unsmoothness of the intensity change may result in the uneven sputtering rate

at the crater in addition to the unstability of the system, even it is not clear. It seems that the longer time interval between onset and offset points stands for the formation of the erratic crater. The time during the appearance of nickel singal represents the sputtering time for the only nickel coated on the copper.

In the Figure 13, the plotting of the coating thickness of sample used *vs* sputtering time required makes it possible to estimate the sputtering rate of this system. The estimated sputtering rate is 0.2 μm/min, which is close to the reported under the similar operating condition. Unfortunately, the depth profile using the pin type ion source was not studied, so that it is impossible to compare the performance of the two different types of ion source.

References

1. D. C. Duckworth and R. K. Marcus, *Appl. Spectrosc.,* **44,** 649 (1990).
2. D. C. Duckworth and R. K. Marcus, *Anal. Chem.,* **61,** 1879 (1989).
3. J. C. Belle and J. D. Johnson, *Applied Spectroscopy,* **27,** 118 (1973).
4. J. E. Greene and F. Sequeda-Osorio, *J. Vac. Sci. Technol.,* **10,** 1144 (1973).
5. J. E. Greene and F. Sequeda-Osorio, *Appl. Phys. Letters,* **25,** 435 (1974).
6. J. E. Greene and J. M. Whelan, *J. Appl. Phys.,* **44,** 2509 (1973).
7. J. E. Greene, F. Sequeda-Osorio, and B. R. Natarajan, *J. Vac. Sci. Technol.,* **12,** 366 (1975).
8. M. E. Waitlevertch and J. K. Hurwitz, *Applied Spectroscopy,* **30,** 510 (1976).
9. J. Pons-Corbeau, *Surf. Interace Anal.,* **7,** 169 (1985).
10. J. Pons-Corbeau, J. P. Cazet, J. P. Moreau, R. Berneron, and J. C. Charbonnier, *Surf. Interace Anal.,* **9,** 21 (1986).
11. A. Bengton, *Spectrochim. Acta* **40B,** 631 (1985).
12. H. Nickel, D. Guntur, M. Mazurkiewicz, and A. Naoumidis, *Spectrochim. Acta.,* **46B,** 125 (1991).
13. M. Hecq, A. Hecq, and M. Fontingnies, *Anal. Chim. Acta,* **155,** 191 (1983).
14. M. V. Straaten, A. Vertes, and R. Gijbels, *Spectrochim. Acta,* **46B,** 283 (1991).
15. K. B. Lee, D. W. Moon, and D. W. Lee, *Bull. Korean Chem. Soc.,* **6,** 524 (1989).
16. K. B. Lee, H. J. Kim, C. J. Park, D. W. Moon, and K. W. Lee, *Analytical Science & Technology,* **3,** 215 (1990).